THE DYNAMICS OF A LASER PRODUCED HEAVY ION PLASMA.

Lawrence Martin Schadegg

United States
Naval Postgraduate School

THESIS

THE DYNAMICS OF A LASER
PRODUCED HEAVY ION PLASMA

by

Lawrence Martin Schadegg

June 1970

The Dynamics of a Laser Produced Heavy Ion Plasma

by

Lawrence Martin Schadegg
Lieutenant (junior grade), United States Navy
B.S., United States Naval Academy, 1969

Submitted in partial fulfillment of the
requirements for the degree of

MASTER OF SCIENCE IN PHYSICS

from the

NAVAL POSTGRADUATE SCHOOL
June 1970

ABSTRACT

To investigate the front of a laser produced plasma that is expanding in a homogeneous magnetic field a reliable method of positioning the target, monitoring the laser, and observing the properties of the expanding plasma had to be developed. Photodiodes and supporting circuitry were constructed to observe the laser interaction with the plasma, plasma expansion velocity, and total light emitted from the plasma. A heavy material, copper, was chosen to slow down the processes occurring in the expanding plasma front.

The predictions of a computer program of the mathematical analogue to the experiment give expansion velocities of $\sim 10^6$ cm/sec and indicate a bouncing of the plasma front off the magnetic field.

TABLE OF CONTENTS

LIST OF ILLUSTRATIONS

ACKNOWLEDGEMENT

There have been many people involved in this project to whom I owe the deepest appreciation. I would like to principally thank Mr. Hal Herreman for his assistance in the laboratory no matter the hour of day, Mr. Michael O'Dea for his aid in making abstract drawings become mechanical realities, Professor Alfred Cooper for his assistance in the program, and Professor Fred Schwirzke for his constant drive into the unknown and his patience in explaining the theory.

My warmest appreciation goes to my wife Peggy for her support and long typing hours in the past year.

I also wish to thank the Air Force Office of Scientific Research without whose contract (#MIPR 69-0004) this experiment could not have been undertaken.

I. INTRODUCTION

This experiment was the first in a series that will ultimately end in the study of collisionless shock waves propagating in a steady state plasma. The primary aim of this project was to set up an experiment by which the expansion of a plasma in a magnetic field is studied with primary interest being in the propagation of the front of the plasma.

The primary component of the experiment is the plasma facility at the Naval Postgraduate School. The target wire is held in the chamber that is evacuated to about 10^{-6} torr. A homogeneous magnetic field (variable up to 10KG) is impressed along the axis of the column. The laser is focused on the target, a metallic wire fiber, and the target is vaporized and ionized. The resultant plasma begins to expand under the force of the interior pressure gradients generated by the heating of the laser.

The expanding front of the plasma is studied by means of magnetic probes, electrostatic double probes, photodiodes and the calorimeter.

II. THEORY

The problem of producing a plasma by irradiating a small solid mass with a laser has inherent conditions that allow a theoretical model of expanding plasma to be developed.

Since the amount of energy required to vaporize the small mass is so much smaller than that energy required to ionize the atoms, it is safe to assume for one of the initial conditions that at immediately after time t = o, when the laser fires, there exists a small sphere of plasma approximately the size and density of the original solid particle.

The relaxation time for a 90° deflection caused by coulomb interactions between the ions and electrons is given by

$$\tau_{e\text{-}i} = 1.3 \times 10^{5} \frac{T^{3/2}}{Z \ln \Lambda} \qquad (1)$$

Given below are the approximate conditions for the plasma the experiment was concerned with

$$T \simeq 10 ev \ , \quad \eta \simeq 10^{21} cm^{-3} \ , \quad \ln \Lambda \simeq 10 \qquad (2)$$

then for these conditions

$$\tau_{e\text{-}i} = 3.9 \times 10^{-16} sec \qquad (3)$$

The approximate time increment (τ) for the plasma wave front to move one focal diameter is used as the characteristic time for the plasma. This time is on the order of 10^{-9} sec. Since $\tau_{e\text{-}i} << \tau$ a hydrodynamic treatment of the problem can be used.

John Dawson's paper[1] treats the case of a freely expanding plasma. This paper gives a very good foundation upon which to base further theory. From his theory it is the next logical step to treatment of a plasma in a magnetic field.

By considering just the principle of energy conservation, we can arrive at the first equation we will use in the theoretical treatment of the plasma. We have

Thermal Energy + Expansion Energy - Radiation losses - Particle losses = Energy supplied by laser (4)

The particle losses are considered to have only long time effects and will not be included at this time.

The first two terms have incorporated into them the plasma interaction with the magnetic field term. Part of the interaction term adds to the thermal energy due to joule heating, but the effect on the second term is more complicated. As the plasma expands the thermal energy is converted to expansion energy, the expansion of the surface causes potential energy to be stored in the magnetic field. The magnetic field eventually pushes back the plasma and an oscillatory motion about the $\beta = 1$, plasma pressure = magnetic pressure, position is started. Assuming each term in the energy equation

---

[1] Dawson, J. M., "On the Production of Plasma by Giant Pulse Lasers," The Physics of Fluids, v. 7, p. 981, July 1964.

is initially zero at time t = 0 the two derivatives of the above quantities can also be equated.

The thermal energy is

$$\frac{3}{2} NKT \tag{5}$$

Where N→number of ions and number of electrons produced.

The time rate change of the thermal energy is

$$\frac{3}{2} Nk \frac{dT}{dt}$$

Expansion energy is given by

$$\frac{1}{2} m \dot{R}^2 \tag{6}$$

Where m is average total mass, R is the radial vector component of the plasma front.

The derivative becomes

$$\frac{1}{2} m \frac{d}{dt} \dot{R}^2 \tag{7}$$

but this is the work dissipated in the change in volume or

$$\frac{1}{2} m \frac{d\dot{R}^2}{dt} = \frac{d(PV)}{dt} = V \frac{dP}{dt} + P \frac{dV}{dt} \tag{8}$$

Where P is the plasma pressure,
V is the plasma volume.

At this point we assume a spherical symmetric plasma. This assumption is not apparently valid for the plasma of the experiment due to two reasons:

1. The different expansion velocities along and across the field lines could cause asymmetry.

2. We are irradiating the end of a cylindrical fiber with the laser and not a small round pellet.

We justify the first assumption by the following. The plasma is initially dense enough to almost completely exclude the magnetic field and will behave as a free expanding plasma as long as $\beta >> 1$, which is the condition in the initial stages of the expansion. For the second case the laser intensity was assumed to have a flat Gaussian shape over the focal diameter. By centering the focal spot on the end of the fiber the length of the wire to be irradiated is know and only one of the gradually tapering tails on the intensity cross section of the beam comes into play. (See Fig. 1). It is this tail that generates whatever unionized atoms that may exist, due to the insufficient power densities. By only having one side of the focal spot intersecting the target the number of unionized atoms are minimized. The presence of the wire target does not have much effect for two reasons.

1. The target diameter, about 25μ, is very much smaller than the radius, about 1 cm., of the plasma at the time when the measurements are made.
2. A potential sheath is developed around the wire as the plasma expands shielding the plasma from the wire target.

Then, assuming a spherical plasma the volume is

$$V = \frac{4}{3} \pi R^3 \tag{9}$$

or

$$\frac{dV}{dt} = 4 \pi R^2 \dot{R} \tag{10}$$

then

$$V\frac{dP}{dt} + P\frac{dV}{dt} = \frac{4}{3}\pi R^3 \frac{dP}{dt} + P4\ R^2\dot{R} \tag{11}$$

But the pressure P is given by

$$P = \frac{NkT}{V} = \frac{3NkT}{\pi 4R^3} \tag{12}$$

So when the time derivative of the expansion energy term becomes

$$Nk\frac{dT}{dt} + 3NkT\frac{\dot{R}}{R} \tag{13}$$

The interaction term between the magnetic field and the expanding plasma of earlier is just the resistivity of the plasma multiplied by the current squared generated on the surface by the magnetic field interaction. The energy change per unit time per unit volume is:

$$W_{(\text{interaction})} = \eta j^2 \tag{14}$$

Where η is the resistivity,
j the current.

Now if we assume that the electric fields are slowly varying then we can write that

$$|j| = \vec{\nabla} \times \vec{B} \tag{15}$$

Assuming that the magnetic field has an exponential decay into the plasma with an e^{-1} penetration distance of λ (skin depth).

The expression for the magnetic field becomes:[2]

$$B = B_o \, e^{-r/\lambda} \tag{16}$$

Where B is the magnetic field in the plasma,
B_o is the exterior magnetic field at the plasma boundary.

$0 < r < R$

From Maxwell's equation the current is found

$$\vec{j} = \vec{\nabla} \times \vec{B} = \frac{-B}{4\pi\lambda} e^{-r/\lambda} \tag{17}$$

To find the total change of energy per unit time for the plasma volume the above is integrated over the plasma volume.

$$\int_0^R \eta j^2 dV = \int_0^R \eta \frac{B^2}{\lambda^2} \frac{4\pi x^2}{(4\pi)^2} e^{-2(R-x)/\lambda} \, dx$$

$$= \frac{\eta B^2}{\lambda^2 4\pi} e^{2R/\lambda} \int_0^R x^2 e^{2x/\lambda} \, dx$$

$$= \frac{\eta B^2}{8\pi\lambda} \left[(1 - e^{-2R/\lambda})(R^2 - R\lambda + \frac{\lambda^2}{2}) \right] \tag{18}$$

The primary radiation loss mechanism is due to Bremsstrahlung. The power loss is given by Glasstone and Loveberg[3] as:

---

[2] Bhadra, D. K., "Expansion of a Resistive Plasmoid in a Magnetic Field," The Physics of Fluids, v. 11, p. 235, January 1968.

[3] Glasstone, S. and Lovberg, R. H., "Controlled Thermonuclear Reactions, p. 30, D. Van Nostrand Company, Inc., 1960.

$$P_{br} \simeq \frac{16\pi (kT)^{3/2} \eta_e \eta_i Z^2}{\sqrt{3}\, m_e^{3/2} c^3 h} \qquad (19)$$

Where ηe, ηi are the electron and ion densities respectively.

Z is the charge per ion

kT is the electron temperature in ev

The expression for the power supplied by the laser is found in a paper by Haught and Polk.[4]

$$W(t) = \begin{cases} \theta(t) \left(\frac{R}{\Gamma}\right)^2 (1 - e^{KR}) & R \leq \Gamma \\ \theta(t)(1 - e^{KR}) & R > \Gamma \end{cases} \qquad (20)$$

Where $\theta(t)$ is the laser power as a function of time (usually Gaussian form)

Γ is the radius of the focal spot.

R is the radius of the plasmoid.

K is the absorption coefficient given by Dawson and Oberman.[5]

$$K = \frac{80 Z^2 e^6 \pi \eta_e \eta_i}{c v^2 (2\pi m kT)^{3/2}} \qquad (21)$$

collecting all the terms the equation for the change of energy per unit time becomes:

---

[4] Haught, A. F. and Polk, D. H., "High-Temperature Plasmas Produced by Laser Beam Irradiation of Single Solid Particles," The Physics of Fluids, v. 9, p. 2451, October 1966.

[5] Dawson, J. M. and Oberman, C., "High-Frequency Conductivity and the Emission and Absorption Coefficients of a Fully Ionized Plasma," The Physics of Fluids, v. 5, p. 520, May 1962.

$$\frac{5}{2}Nk\frac{dT}{dt} + \frac{3NkT}{R}\frac{dR}{dt} - \frac{16\pi(kT)^{3/2}Z^2}{3(m_e)^{3/2}c^3h}\eta_e\eta_i -$$

$$\frac{\eta B^2}{n\lambda}\left[(1-e^{-2R/\lambda})(R-R\lambda+\lambda^2/2)\right] = W(t)$$

(22)

The second equation needed is the linearized MHD equation that governs the plasma dynamics.

$$\rho\frac{d\vec{V}}{dt} = \vec{\nabla}P - \frac{(\vec{j}\times\vec{B})}{c} \tag{23}$$

Under the same assumptions used earlier along with the assumption that the pressure goes linearly to zero at the boundary of the plasma, the equation (23) becomes:

$$\frac{d}{dt}\left[\frac{1}{2}m\dot{R}^2\right] = \frac{P_{total}}{R}\dot{R} - \int_V \frac{j\times B}{c}\dot{R}\,dV \tag{24}$$

or

$$\frac{1}{2}m\frac{d\dot{R}^2}{dt} = \frac{NkT}{R}\dot{R} - \frac{1}{c}\int_V (j\times B)\dot{R}\,dV \tag{25}$$

from before $B = B_o e^{-r/\lambda}$

and $j = \nabla \times B = \frac{B}{4\pi x} e^{-r/2}$

then

$$\frac{1}{c}\int_0^R (j \times B)dx\ \dot{R} = \frac{B^2}{c}(1-e^{-R/\lambda})(R^2-2R\lambda+2\lambda^2)\dot{R} \tag{26}$$

equation (25) becomes

$$\frac{1}{2}m\frac{d(\dot{R}^2)}{dt} = \frac{NkT}{R}\dot{R} - \frac{B^2}{c}(1-e^{-R/\lambda})(R^2-2R\lambda+2\lambda^2)\dot{R} \tag{27}$$

The third equation is derived from the linkage of the electric field on the surface to the magnetic field. The change in flux (Φ) in time is equal to the line integral of the electric field in the moving frame (Em).

$$\dot{\Phi} = -\int \vec{E}_m \cdot d\vec{l} \tag{28}$$

$$\vec{E}_m = \vec{E} + \frac{\vec{v}}{c} \times \vec{B}$$

by generalizing Ohm's law and neglecting the electron pressure gradient we have

$$-\int\left(\frac{1}{\omega_{pe}^2}\frac{d\vec{j}}{dt} + \eta\vec{j}\right)\cdot d\vec{l} = \dot{\Phi} \tag{29}$$

We consider only those components of j that are parallel to the surface of the expanding plasma and drop the $\frac{dj}{dt}$ term since it turns out to be too small to consider. We now have

$$\frac{d\Phi}{dt} = -\int \eta \vec{j} \cdot d\vec{l} \tag{30}$$

where Φ , the flux, is given by

$$\Phi = \int_0^R 2\pi B x e^{-(R-x)/\lambda} dx$$

$$\Phi = 2\pi\lambda^2 B \left[\frac{R}{\lambda} - 1 + e^{-R/\lambda}\right] = \frac{\eta R B}{2\lambda} \tag{31}$$

from the expression for j in equation (17) we get

$$\int \eta j \cdot dl = \eta j 2\pi R = \frac{\eta R B}{\lambda 2} = \frac{d\Phi}{dt} \tag{32}$$

then equation (32) becomes

$$\frac{d}{dt}\left[2\pi B\lambda^2 (R/\lambda - 1 + e^{-R/\lambda})\right] = \frac{RB\eta}{2\lambda} \tag{33}$$

The resistivity is given by Spitzer[6] to be

$$\eta = 5.2 \times 10^6 \frac{\ln\Lambda}{T^{3/2}} \tag{34}$$

Where T is in electron volts.

The absorption coefficient as derived by Dawson and Oberman[7] was

---

[6] Spitzer, L., Physics of Fully Ionized Gases, pp. 81-85, Interscience Publishers, Inc., 1956.

[7] Same as Number 5.

$$K = \frac{80Z^2e^6 n_e n_i}{cv^2(2mkT)^{3/2}\pi^{3/2}} \qquad (35)$$

The expression for the skin depth for a stationary wave front found by Fred Schwirzke[8] by setting the magnetic Reynold's number equal to one and using the expression for the conductivity in the classical case. His expression was

$$\lambda = \frac{c^2}{4\pi\sigma v} \qquad (36)$$

where

$$\sigma = \frac{4(8kT)\ 0.683}{(\pi m_e^3)^{1/2}(Ze)^2 \ln\Lambda}$$

The above three equations were programmed by Leslie McKee with the laser power, target material, laser pulse width, laser focal spot size and magnetic field strength as parameters. Some typical results are shown in Fig. 2.

The parameters of the experiment were used in programming the computer. The target material is a wire that is 25μ in diameter and 99.9% pure copper. The focal diameter of the laser was measured to be about 800μ in diameter and if the focal spot is centered on the tip of the fiber, about a 400μ

---

[8] Schwirzke, F. and Tuckfield, R. G., "Observation of Enhanced Resistivity in the Wave Front of a Laser-Produced Plasma Interacting with a Magnetic Field," Physical Review Letters, v. 22, p. 1287, June 1969.

length of the wire is converted to plasma. The pulse width of the laser was 19 nsec and laser energy output was about 200 joules. The plasma facility has the capability of producing a homogeneous magnetic field of values from 0 to 10KG. The value used in the program was 5KG. The copper was assumed to be doubly ionized. The calculated necessary energy conditions to achieve this were met in the plasma. The computer program does not take into account the particle losses along the magnetic field but this will cause a variation mainly in the time base of the results and not the properties of the results, i.e., the bouncing, will occur earlier.

In general the results were that for the free expansion case the expansion velocity of plasma approached an asymptotic limit dependent on the parameters above; confirming Dawson's results that the temperature decreases monotonically after the laser is shut off,[9] which is not the case if the plasma is in a magnetic field. Then the temperature would be higher due to the heating that occurs while working against the magnetic field. In the case of the plasma expanding in a homogeneous magnetic field the plasma expands to a radius until $\beta \simeq 1$. Then the plasma is pushed back by the magnetic field (bounced) to a radius somewhat less than the equilibrium position of $\beta \simeq 1$. As the plasma was pushed back it was adiabatically

---

[9] Dawson, J. M., "On the Production of Plasma by Giant Pulse Lasers," The Physics of Fluids, v. 7, p. 985, July 1964.

heated so a point would be reached where the magnetic field stops pushing and begins to expand again, but in expansion there were two competing processes going on, one was the adiabatic cooling due to expansion, and the other was the resistive heating due to the interaction of the expanding front with the magnetic field. The resistive heating implies a diffusion of the plasma to a larger radius on the second bounce but is pushed back past where $\beta=1$ as occurred after the first bounce. The plasma radius varies sinusoidally but with an envelope that asymptotically approaches a limit, the same as the results predicted by Bhadra.[10] A question raised was: exactly to what extent do the various mechanisms in the heating and cooling of the expanding plasma take effect? This question was partly prompted by the results of Fred Schwirzke's work at General Atomic.[11] He noted that after a long time and at a large radius the plasma structure took on a smoke ring shape. The process that may cause this was not completely understood. One possible mechanism that had been brought forward had to do with the $\frac{1}{B^2}$ dependence of the coefficient of heat conductivity that exists in plasma. Initially when the plasma was formed there was a slight penetration of the magnetic field due to the finite resistivity of the

---

[10] Bhadra, D. K., "Expansion of a Resistive Plasmoid in a Magnetic Field," The Physics of Fluids, v. 11, p. 237, January 1968.

[11] Schwirzke, F. and Tuckfield, R. G., "Dynamics of a Laser Created Plasma Expanding in a Magnetic Field," Plasma Physics, v. 11, p. 12, Pergamon Press, 1969.

plasma when the temperature was still low. As the plasma expanded the trapped magnetic field inside reduced the heat conductivity inside sufficiently such that there was reduced heat transport towards the center. The heating that occurred in the front due to the interaction with the magnetic field did not have time to spread evenly throughout the plasma volume. This caused a concentration of the heat in the outer volume of the plasma sphere forming a shell. This geometry was probably reduced to a ring form since the plasma expanding along the field lines escaped and only the annular plasma expanding across the field lines remained.

Another question raised was, is there some heating mechanism in a freely expanding plasma that has not been considered? For example, the plasma could be in a turbulent state similar to the problem dealt with by Sagdeev in his paper on cooperative phenomena,[12] and have pressure and temperature gradients that are oriented such as to cause interior currents and magnetic fields in the plasma that could add to the heating of the plasma. This could be investigated by observing the total light from the expanding plasma with a photodiode. The reheating of the plasma would appear as an increase in the light output that is not associated with the laser heating.

---

[12] Sagdeev, R. Z., "Cooperative Phenomena in Collisionless Plasmas," Reviews of Plasma Physics, v. 4, p. 65-68, Consultants Bureau, 1966.

III. EXPERIMENTAL PROCEDURE

Since the proposed path of experiments leads to the study of shock wave interaction with a steady state plasma column, the plasma facility, a three meter long hollow are cathode discharge at the Naval Postgraduate School, became an integral part of the system. In Fig. 3 the relative placement of the components is shown. The laser is optically coupled to the vacuum chamber through a port that was adapted to hold a 20 cm focal length convex lens and four probes. The center of the vacuum chamber is 20.2 cm from the inside surface of the lens. Across the chamber opposite the lens is a large window and mounted externally to this window is another convex lens of focal about 28 cm. that has its focus spot coincident with the focal spot of the first lens. This lens is to convert the diverging light from the focal point of the first lens to a parallel beam for diagnostics.

Upstream in the chamber a mirror was mounted on the end of a probe and positioned in the chamber such that it was 45° with the axis of the column of the plasma column, enabling a sight to be taken through a port adjacent to the exit port spoke of above and down the axis of the machine perpendicular to the laser axis.

By sighting through two theodolites, one aimed down the axis of the laser and the other into the adjacent port onto the mirror aimed across the axis of the first, we were able

to determine a point in the chamber to be used in positioning the targets later.

A. TARGET ASSEMBLY

The target, a wire fiber, was mounted in a glass holder and the glass holder was mounted in a long metal holder. The assembly (see Fig. 4) was used to position the target from a port above the vacuum chamber down into the beam path. We found that to change the target required about 45 minutes to 1 hour. This was due to the need of bringing the whole vacuum chamber up to atmospheric pressure to remove the target then pumping down to operational pressure, about 10^{-6} torr, when the new target was in place. So the valve system shown schematically in Fig. 4 had to be constructed to allow the target to be changed in only 5 minutes. The target probe holder is mounted above the valve system and will hold a vacuum while the probe is being slid up and down for positioning. To replace the target the target holder with target is slid through the probe holder until it comes into view through the observation window. At this point we also check the condition of the wire to see if it sustained any damage by accidentally being bumped while slid through the seals in the probe holder. Once the target can be seen in the observation window the probe holder is tightened and the valve that leads to the auxiliary rough pump is opened to pump the top chamber down to about 10^{-2} torr. When the thermocouple indicates about 10^{-2} torr, it is safe to open

the large gate leading to the main vacuum chamber. Then the target is slid the rest of the way down into the chamber. The process is reversed to remove the target. The distance from the target probe holder to the center of the chamber is about 30 inches. So to counteract the vibration that might be induced, the metallic probe holder was made of a hollow stainless steel tube. The target does not vibrate except when the holder was being positioned laterally in the chamber and then the vibration damped out quickly.

B. TARGET ALIGNMENT

The glass target holder is replaced in the metal holder with a fitting that holds a 1/4"x1" piece of exposed polaroid film mounted on a piece of glass of like dimensions. This is put into the target chamber such that the surface of the polaroid is 19.9 cm from the face of the lens that focused the laser beam. By aligning a C-W gas laser along the axis of the pulsed laser and shining it through the pulsed laser and the C-W laser beam passes through the focusing lens, the polaroid target is then laterally positioned until the focal spot of the C-W laser is about centered on the polaroid. Then the pulsed laser is fixed and it should hit the film producing a white spot which, if the polaroid is positioned 45^{o} to the axis of the laser, can be seen in both theodolites. Both cross hairs are positioned such that they center on the spot produced by the laser. Caution should be exercised whenever firing the pulsed laser. The theodolites should be shielded such that they do not receive any of the reflected laser beam.

Once the cross hairs of the theodolites are centered on the spot their angular readings are noted for reference.

Now the polaroid target is removed and replaced with a wire target and glass holder. The target is put into the chamber and positioned until the tip of the wire appears at the center of the cross hairs for each theodolite.

C. DETERMINATION OF FOCAL SPOT DIAMETER

Through the use of the theodolites we were able to determine the focal spot size quite accurately. The wire target was replaced with a brittle glass fiber target of known length, then this target was positioned in the chamber such that the center of the fiber was on the center of both theodolite cross hairs. The theodolite on the axis of the laser had its cross hairs moved both vertically and horizontally (the fiber was canted slightly due to method of mounting) so that the center was positioned on one end and then the other. Both horizontal and vertical angular readings were taken and by subtraction we were able to get the arc subtended by the length of the fiber. From this we determined the distance to the fiber from the theodolite pivot point, see Fig. 5a. The cross hairs were then positioned back to their original setting for the focal spot center, and the fiber positioned so that just a small portion of it was below the cross hair center. Then the fiber was moved laterally in small angular increments, of about 10 secs. of arc at a time, across the focal spot and the laser fired, the angular position of the

horizontal scale for the position of the fiber being noted for each firing (see Figs. 5b and 5c). Also whether the target was hit or missed was recorded. The total arc measure from the last miss (one side of the focal spot) to the next miss (the other side of the focal spot) being the angular displacement of the diameter of the focal spot.

The calibrating fiber length (Z) was 45 mm. The arc subtented by the vertical displacement of the fiber (θ_1) was 0.792°, and the horizontal arc displacement due to fiber canting, (θ_2) was 0.0545°. The actual arc displaced by the fiber (θ_3) was given by

$$\theta_3 = \sqrt{\theta_1^2 + \theta_2^2} \text{ or } = 1.384 \times 10^{-2} \text{ radians.} \quad (37)$$

From this, the distance from the fiber to the pivot point of the theodolite (R) was determined to be 325 cm.

As the target was moved laterally across the focal spot the arc (angle) from one miss to the next miss by the laser was 50 seconds or 2.423×10^{-4} radians. This gave us a focal spot size of 0.780 mm. of 780μ.

IV. APPARATUS

A. LASER

The complete laser system consists of an oscillator and an amplifier, but until all the components arrived the oscillator was used by itself utilizing a ruby rod. It was capable of outputting about 200 MW with a 20 nsec pulsewidth.

The oscillator system is shown in Fig. 6 and the electronic flow diagram in Fig. 7. The system is capable of utilizing either Nd-doped glass or ruby lasing material. But a change in some of the optical components is necessary as follows. The front partial reflector of the system is an etalon that is usable for either ruby or Nd-doped glass. The flashtube assembly requires polished aluminum reflectors for the Nd-doped rod and ceramic reflectors for the ruby rod. The Pockels cell has two quartz windows that have anti-reflection coatings with their minimum reflectivity point at some particular frequency. So there are a set for each lasing material. The anti-reflection coatings are facing outward from the cell center and are usually indicated with an arrow pencilled on the side of the quartz window.

In order to use the Nd-doped glass for lasing in the Q-spoiled node a polarizer is required between the laser rod and the Pockel's cell. This polarizer has to be cross-polarized with the brewster stack polarizer that is in between the Pockel's cell and the rear reflector. In our case this polarizer is another brewster stack. The rear reflector is

also a quartz plate, but is coated with a reflective coating that has its maximum reflectivity at a particular frequency. Consequently this too has to be changed for each lasing material.

Some characteristics are listed below.

	Q-switched ruby	3% Nd-doped glass (Schott) --Normal mode
Threshold	3.65 kv or 2664.5 joules	490 kv or 4301 joules
Optimum delay time for Pockel's cell trigger*	1.04 msec	Threshold is too high in this particular glass type to get Q-spoiled mode.
Pulsewidth	19 nsec	
Maximum energy out	4.0 joules; (normal mode 40 joules)	10 joules

The system that is purchased and will be used has one amplifier stage after the oscillator. This amplifier should have an amplification factor of about 20 and will enable us to get into the Gigawatt range in power out. The lasing material for this system is only Nd-doped glass. For conversion to Nd doped glass laser material, all the optical components that are tuned to the 10,600 $\mathring{A}$ wavelength have to be installed; the two Pockel's cell windows with their anti-reflection coatings facing outward and the rear dielectric mirror. Then the laser head is disassembled according to the directions in the manual for the K-1 laser head and the ruby flashlamp

assembly is removed along with the ceramic reflectors. The new flash lamp and aluminum reflectors for Nd are inserted as one unit. The head is reassembled and the Nd-doped glass rod with its pyrex glass shield is inserted. The pyrex shield is needed because the Nd-doped glass is highly susceptible to UV damage (solarization). The complete system is shown in Fig. 8.

The use of the two laser heads with separate flash tube charging and firing networks requires a synchronization. This is the purpose of the delay circuit. This circuit insures that the two firing times of the flashtubes is synchronized and that maximum power is obtained for a given input. The place of the timing circuit is shown in Fig. 8 of the electronic flow of the amplifier-oscillator system. In Fig. 9 is the schematic of the delay circuit and power requirements. The input is the fire signal from the push button of the power supply for the amplifier assembly. There are three outputs. The first is an instantaneous output that is fed to the circuitry for the amplifier head. The other two are both delayed outputs. One is applied to the circuitry of the oscillator laser head; the other is blank. The second delayed output would be used with a laser system that has two amplifier rods. The two delay circuits are identical and are started at the same time. Their delays can be varied from 0.112 msec to 2.622 msec by the delay control potentiometer (full counter clockwise position is minimum delay). The delay

is adjusted by varying the delay potentiometer and observing the energy out with a constant energy from the oscillator. When the maximum output is reached, the delay is adjusted correctly.

1. Alignment

The Nd-doped glass oscillator laser system is set up first and aligned by the methods in the manuals with the Korad mini-autocolumator. The procedure is the same as that described for the ruby except that since there now exists two crossed polarizers in the path to the rear mirror, there will appear very little reflection from the rear mirror. To counteract this, a bias must be placed on the Pockel's cell to permit enough light to penetrate for alignment. Once the oscillator is aligned, the beam expansion optics, needed to expand the beam from the small diameter of the oscillator rod to the larger diameter of the amplifier rod, are mounted on the rail. The concave sides of the lenses face each other. The negative or expansion lens is closest to the oscillator. The two lenses must be 29.4 cm apart. To tell if the negative lens is the one closest to the oscillator, one should take burn patterns at the laser oscillator output and at the beam expansion output. If the burn pattern at the beam expansion output is the larger, the lenses are placed correctly, provided the concave surfaces face each other. These lenses are checked for proper alignment along the axis by using the autocolumator as before, and matching the two reflections with those aligned in the oscillator.

Once the expansion optics are on the rail the amplifier head is placed on and aligned as close as possible with a C-W laser shining from the rear through the rear reflector into the oscillator laser. The brewster cut end is the end that faces away from the oscillator with the laser beam being bent toward the edge that is the longest.

B. MONITORING DETECTOR

The KD-2 detector is a photodiode connected in a circuit that gives two outputs; one, a fast rise time circuit that gives the power curve of the pulse; two, an integrated signal that gives the energy output. The power output of a normal Q-spoiled laser pulse has the form of a Gaussian but the energy output is shown in Fig. 10 where the amplitude a is proportioned to the total energy output of the laser. One method to observe the laser pulse is to take a partial reflection of the beam and reflect it onto a MgO diffuser that reflects 99% of the incident light but reflects it as a point source, that is, spherical waves. The detector is then placed so that it observes the light coming from the diffuser. Since the light being reflected off the diffuser behaves as light emanating from a point source the detector's distance from the diffuser will also determine the level of the signal received due to the $\frac{1}{R^2}$ dependence of the diffused light. This means that whenever any component of the system is moved the output of the laser as seen by the detector must be recalibrated to give a true reading. The K-1 laser system has a

dielectric mirror for the rear reflector. This mirror is not totally reflecting so it is possible to monitor the beam by placing the detector behind the laser. Now since the beam is not diffusing there no longer exists any distance parameter in the calibration of the detector's output. The optimum signal was obtained by using a neutral density filter of index 1.00 or 2.00 in front of the detector. Assuming about 0.1% light leakage from the rear mirror of the laser the power observed is about 10^{-5} of the laser output power.

The detector is calibrated by its use in conjunction with a calorimeter. The calorimeter gives us the total energy in the laser beam, so by comparing the two energy readings from the calorimeter and the detector's integrated signal it is possible to come up with a linear relationship that gives the laser output energy knowing the output value of the detector's energy signal.

The calibration setup is shown in Fig. 11. The procedure was performed several times with typical calibration curves and data in Fig. 12. Once the output of the detector is calibrated the detector is permanently mounted on the rear of the laser to monitor each shot of the laser to get the energy and peak power for each shot. This monitoring is necessary to insure that the laser is performing correctly from shot to shot. Since the photo diode is strongly frequency dependent (See Fig. 13 a calibration must be performed on each lasing material.

C. CALORIMETER

The Korad calorimeter measures the total energy of the laser beam by measuring the amount of heat absorbed due to the laser beam heating. A typical experimental setup is shown in Fig. 11.

Two things must be kept in mind in its use:

1. The output calibration figure, 1 μ V out for each 0.2 joule of energy absorbed, is temperature dependent. Under normal operation, however, i.e., room temperature, laser fired about once every 2-3 minutes, the maximum variation of the output was 11% for a maximum variation of the laser energy, as read by the detector of 1%.

2. The calorimeter, KJ-3, is for high energy levels and does not represent a very reliable reading for laser energies below 1 joule.

D. MAGNETIC PROBES

The primary diagnostic tool will be the magnetic probe. It is composed of a coil of wire enclosed in a glass sheath and should have a very complete cable shielding system. From magnetic probes, information on the plasma current density, resistivity, kinetic pressure, and average particle density can be found.

The voltage (V) induced in the coil is given by

$$V = nA \frac{dB}{dt} \tag{38}$$

Where n number of turns in the coil
A cross sectional area of coil
B magnetic field parallel to the coil's axis

To obtain the magnetic field we have to integrate the magnetic probe signal with respect to time. This is accomplished by taking the output of the coil across an integrating R-C circuit where the R-C time constant $\tau \gg \tau_c$, the characteristic time of the phenomena under consideration. Then

$$V = \frac{nAB}{R_T C_T} \tag{39}$$

Where the subscripts T refer to total quantities. There are inherent resistances and capacitances in the probe besides the integrating network that may have to be included. Usually the inherent resistance and capacitance is very much less than the integrating circuit values so they can be omitted. From Maxwell's equations we find the current density

$$\vec{\nabla} \times \vec{B} = \vec{j} + \varepsilon \frac{d\vec{E}}{dt} \tag{40}$$

if we assume that the electric field changes little in time then

$$\vec{\nabla} \times \vec{B} = \vec{j} \tag{41}$$

The orientation of the probe coil determines what field component we measure. The direction of the component is the direction parallel to the axis of the coil. Now if we measure the magnetic field components in the right directions to

arrive at the quantities E, (the E field is arrived at by the use of a double probe) and j that are both in the same direction we can find the conductivity from

$$\sigma = \frac{j_1}{E_1} \tag{42}$$

The subscript signifies direction.

The kinetic pressure is found from

$$\vec{j} \times \vec{B} = \frac{\vec{\nabla} P}{R} + \rho \frac{d\vec{V}}{dt} \tag{43}$$

Now if ρ , the density, is small enough we can neglect the $\rho \frac{dV}{dt}$ term, and assuming P has some reference pressure that we set equal to zero at the plasma tube wall then

$$\frac{\vec{P}}{R} = \vec{j} \times \vec{B} \tag{44}$$

The density is found from the equation of state for an ideal gas, where the density ρ and temperature T are functions of the radius

$$P = \rho(r)\, k\, T(r) \tag{45}$$

E. PHOTODIODES

We have two uses for photodiodes in this experiment. One is to put four diodes in a line and place them all outside of the exit port and in the parallel beam made by the lens that is focused on the laser focal spot. They are then effectively looking at different radii of the plasma expansion. By observing how the laser light pulse is affected by the expanding plasma we can observe the relative power of the laser beam with and without the plasma and get a figure

of the energy absorbed in creating the plasma. A time history of the absorption process also becomes available. The expansion velocity could be determined from comparison of the different diode outputs. The second use was to put one of these pin diodes in a glass sheath and put it in the vacuum chamber in such a position that it observes the light emitted from the plasma itself, thereby giving us a method to observe the plasma as a function of time due to the varying light intensity outputs.

Since the 4 diodes in the beam will be absorbing considerable amounts of power from the pulsed laser it will be necessary to filter the incoming light somewhat.

The conditions that the current and voltage and power in the diode must meet are:

$$\text{I.}\quad I_{p_{ave}} E_p < 0.1\text{w} \tag{46}$$

$$\text{II.}\quad I_{p_{peak}} < \frac{I_{p_{ave}}}{(\text{prf})\,(\text{pulse duration})}$$

or

$$< \frac{1000\ \text{Amp}}{(\text{pulse duration})}$$

or

$$< 500\ \text{mA}$$

Where E_p is the supply bias voltage

I_p is the photodiode current.

letting

$$E_p \simeq -20v$$

Pulse duration $\simeq$ 20ns

$$prf \simeq \frac{1 \text{ pulse}}{120 \text{ sec.}}$$

these conditions reduce to

$$I_{p_{peak}} < 500\,ma \tag{47}$$

and

$$I_{p_{ave}} < 5\,ma \tag{48}$$

The response of the diode of 7700 $\mathring{A}$ is 0.5 $\frac{\mu A}{\mu W}$. Corrected to a wavelength of 6943 $\mathring{A}$ the response becomes 0.4 $\frac{\mu A}{\mu W}$

Now the above conditions become

$$W_{p_{ave}} < 12.5\,mw \tag{49}$$

and

$$W_{p_{peak}} < 1250\,mw \tag{50}$$

The total laser output is on the order of 2×10^6 W so a filtering system (neutral density) with index 8 will be required to protect the diodes.

This is a maximum value now since the laser light will be spread over an area of 6 cm^2 and the surface area of the diode is only 3×10^{-2} cm^2. We see that the energy received is only about 5×10^{-3} of the total. The filter index could

be reduced to 5 but to prevent damage to the diodes it is best to start with the denser filtering. These diodes are very frequency sensitive, so the response is different for each frequency. Figure 14 gives the relative spectural response of the diodes. The two correction factors of interest are:

for

$\lambda = 10600$ Å correction factor = 0.3

$\lambda = 6943$ Å correction factor = 0.8

It is this correction factor that is multiplied by the response of the diode at 7700 Å to obtain the real response at the frequency in question. To get the optimum rise time of the diode output, each diode was incorporated in the circuit shown in Fig. 14. The rise time for this circuit is nominally 15 - 20ns for a 10ns input, so the diodes can follow the laser output.

Due to the lens that is an inherent point of these diodes they have a beam width of about 20 deg. through which they can receive a signal.

V. CONCLUSION

With the expectant results, as obtained from the mathematical treatment of the experimental situation, serving as governing parameters for the construction of the experimental apparatus, the information needed for investigation of the expanding plasma should be readily attainable. The experimental parameters, such as focal spot size, amount of target ionized, laser power and energy are determined. Time precludes the inclusion of experimental measurements on the expanding plasma but the method of the experiment is set and can be readily continued.

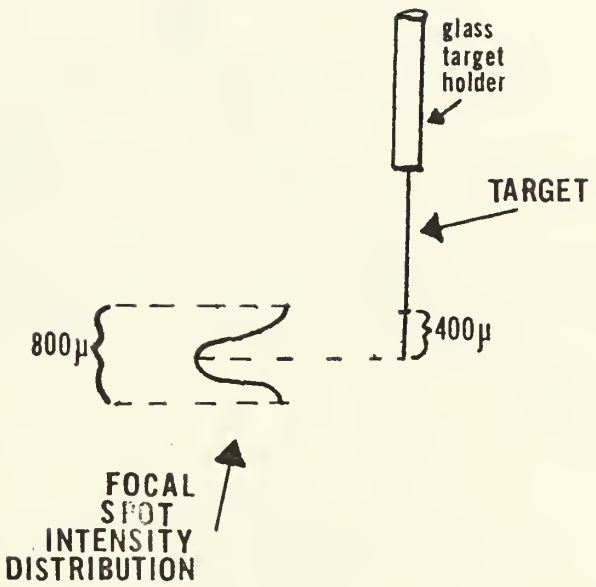
glass
target
holder
TARGET
800μ
400μ
FOCAL
SPOT
INTENSITY
DISTRIBUTION

fig.1

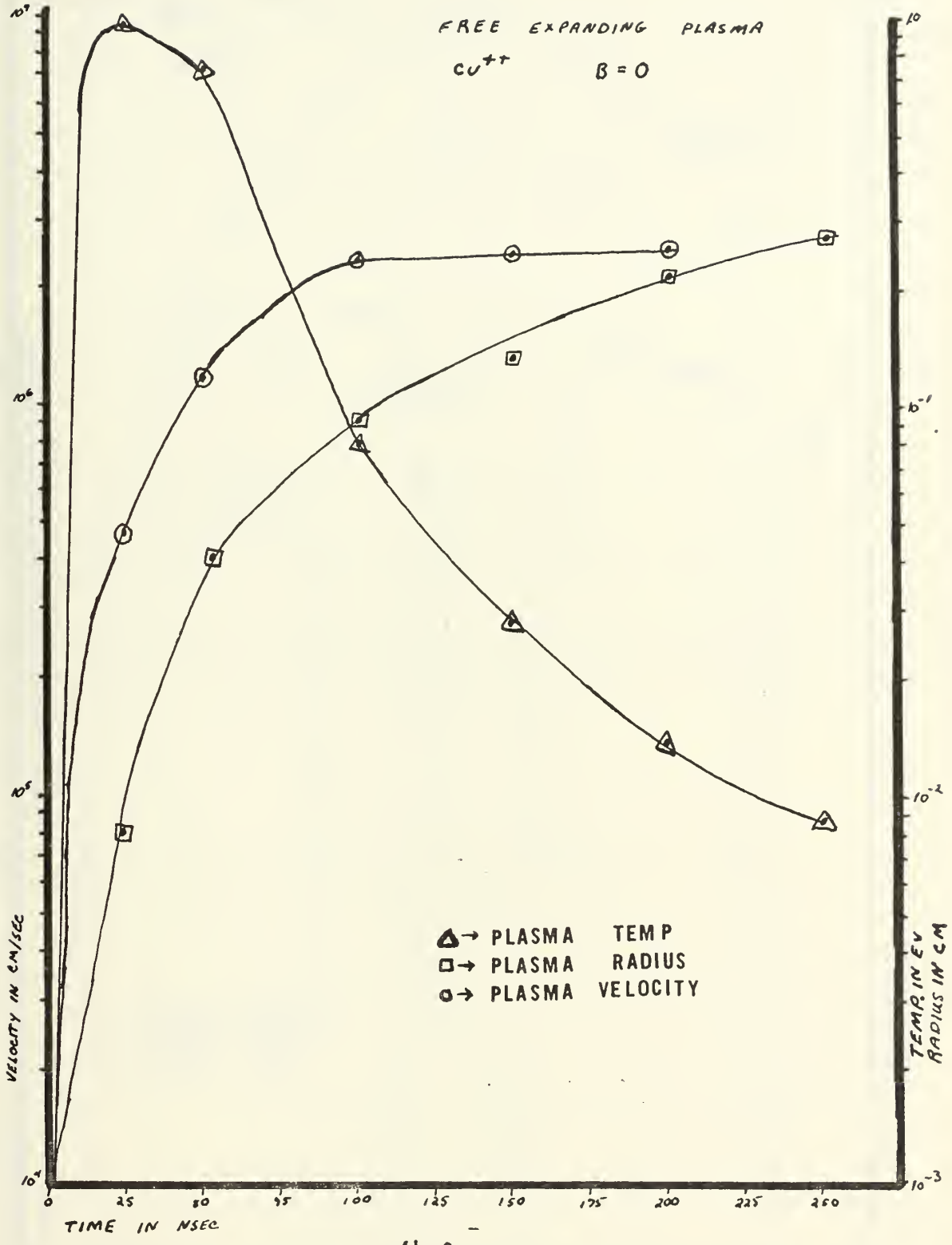
FREE EXPANDING PLASMA
Cu^{++} $\beta = 0$
10^7
10^6
10^5
10^4
VELOCITY IN CM/SEC
10
10^{-1}
10^{-2}
10^{-3}
TEMP. IN EV
RADIUS IN CM
0 25 50 75 100 125 150 175 200 225 250
TIME IN NSEC
△→ PLASMA TEMP
□→ PLASMA RADIUS
○→ PLASMA VELOCITY

Fig.2a

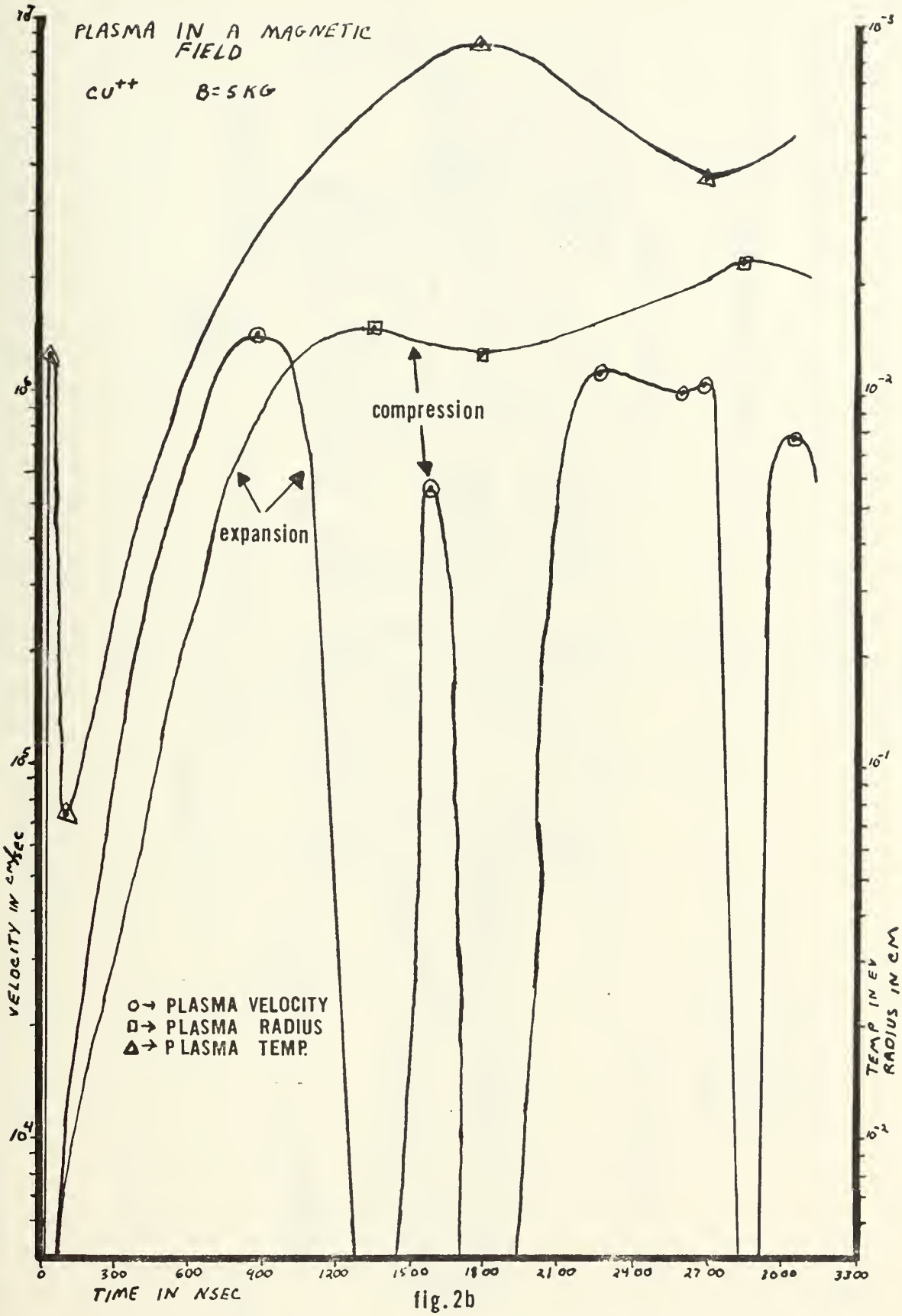
PLASMA IN A MAGNETIC FIELD
Cu^{++} B=5KG
compression
expansion
O→ PLASMA VELOCITY
□→ PLASMA RADIUS
Δ→ PLASMA TEMP.
VELOCITY IN CM/SEC
TEMP IN EV
RADIUS IN CM
0
300
600
900
1200
1500
1800
2100
2400
2700
3000
3300
TIME IN NSEC

fig. 2b

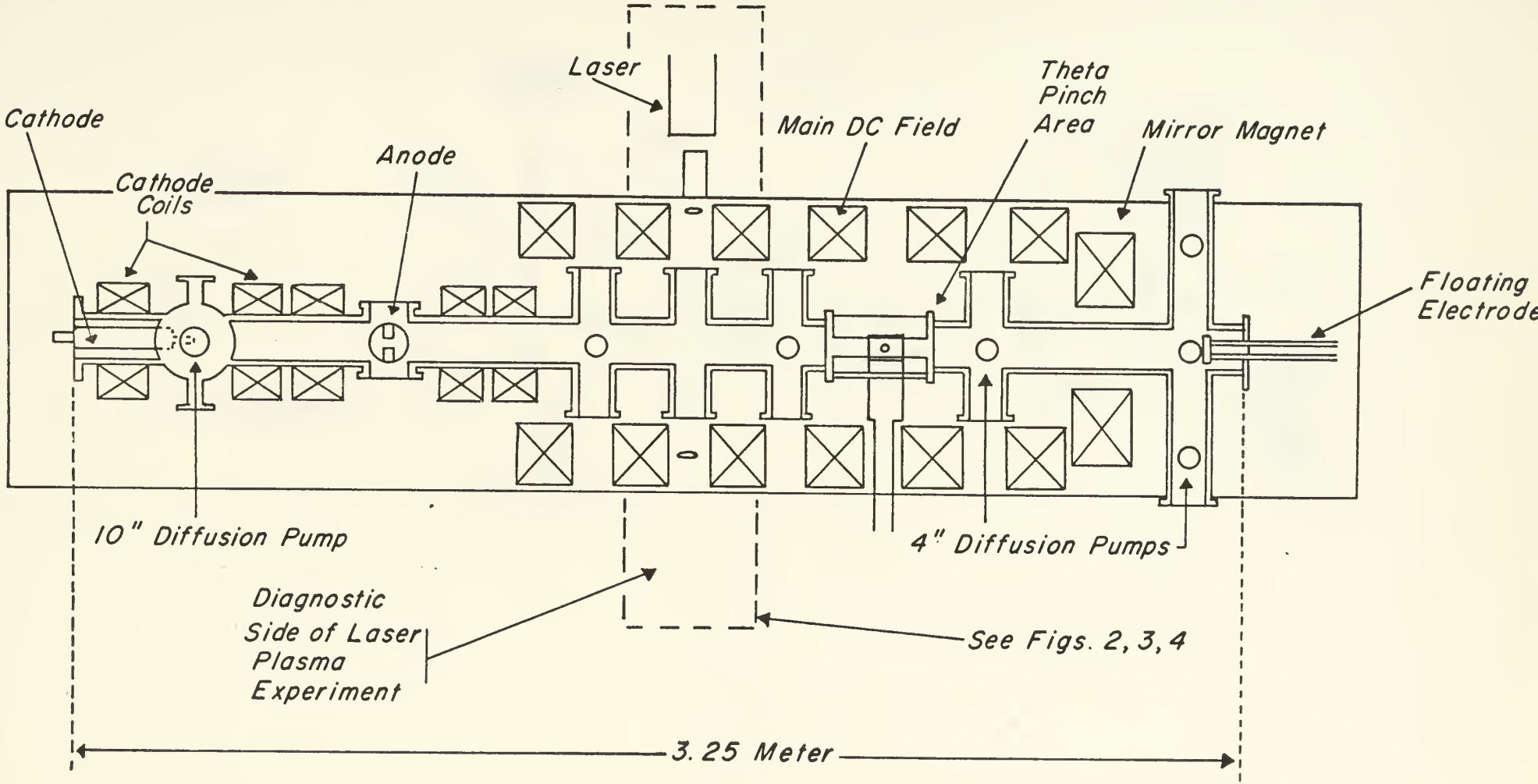

FIG.3a
TOP VIEW OF PLASMA STUDY FACILITY

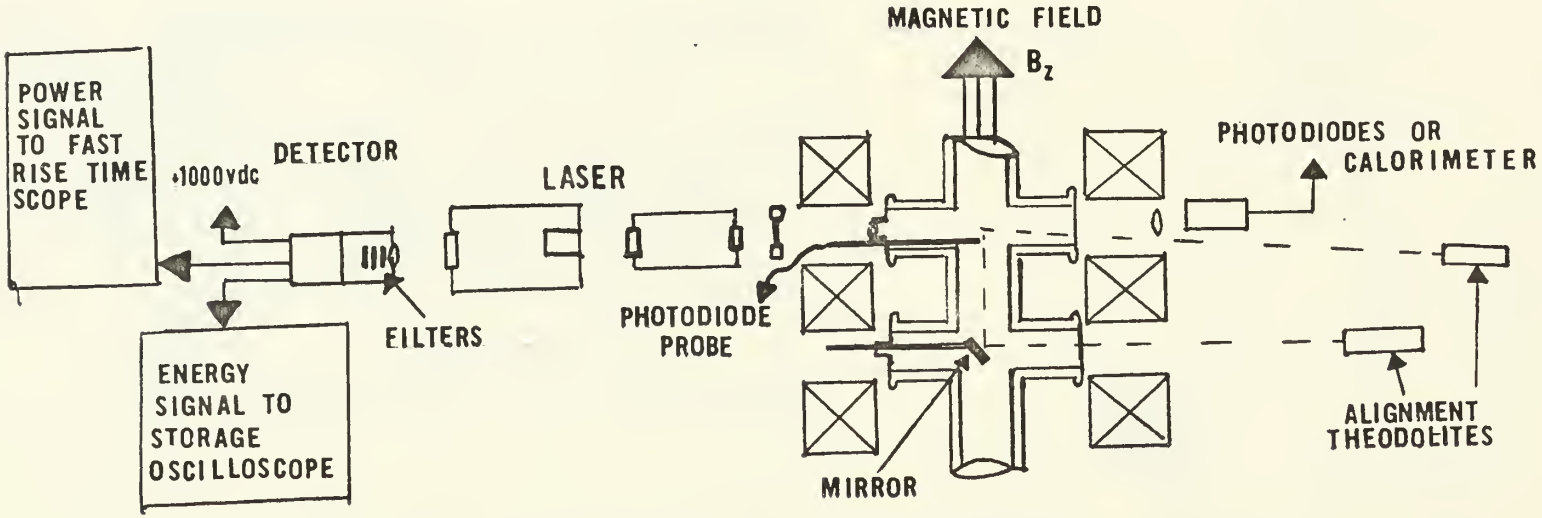
MAGNETIC FIELD
B_z
POWER SIGNAL TO FAST RISE TIME SCOPE
+1000vdc
DETECTOR
LASER
PHOTODIODES OR CALORIMETER
FILTERS
PHOTODIODE PROBE
ENERGY SIGNAL TO STORAGE OSCILLOSCOPE
ALIGNMENT THEODOLITES
MIRROR
VACUUM CHAMBER

fig.3b

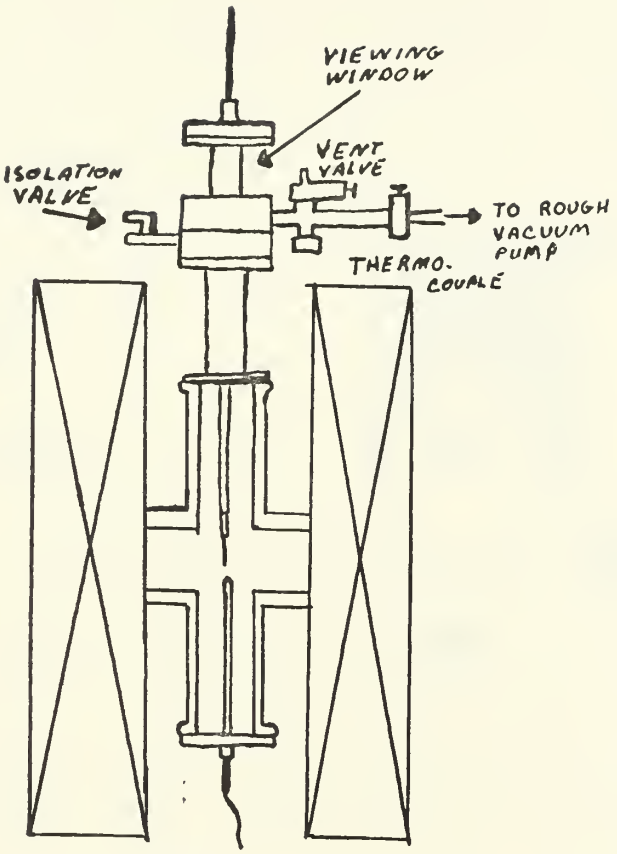
VIEWING WINDOW
VENT VALVE
ISOLATION VALVE
TO ROUGH VACUUM PUMP
THERMO-COUPLE

fig.4

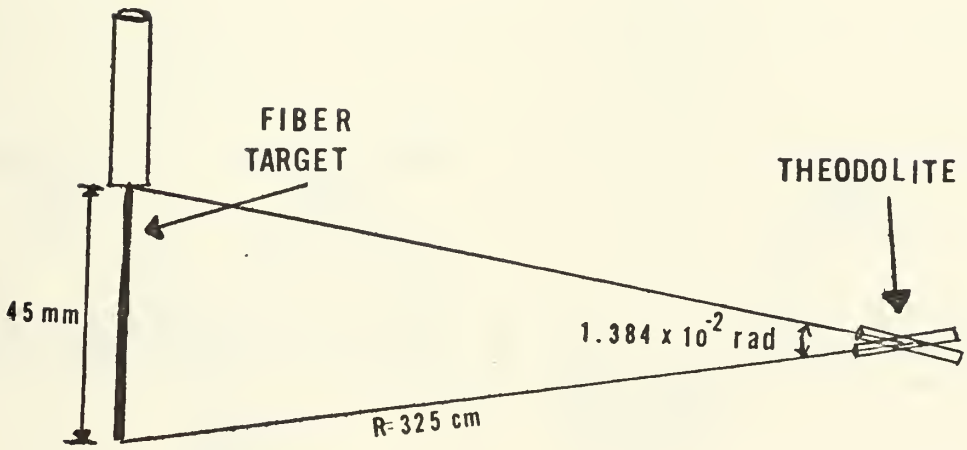
FIBER TARGET
THEODOLITE
45 mm
1.384 x 10^{-2} rad
R=325 cm

fig. 5a

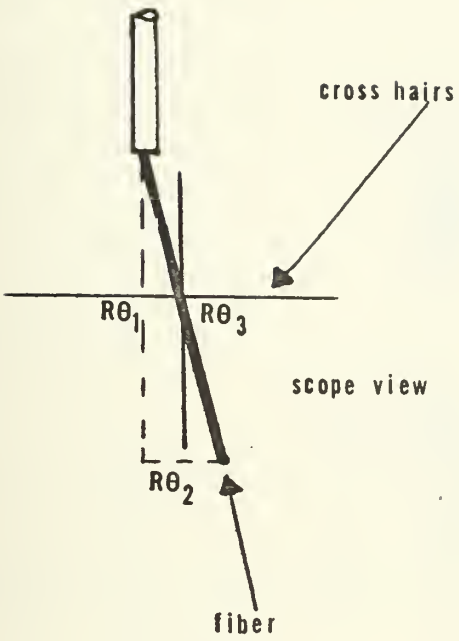

fig. 5b

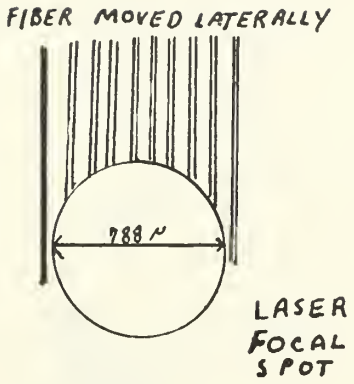

fig.5c

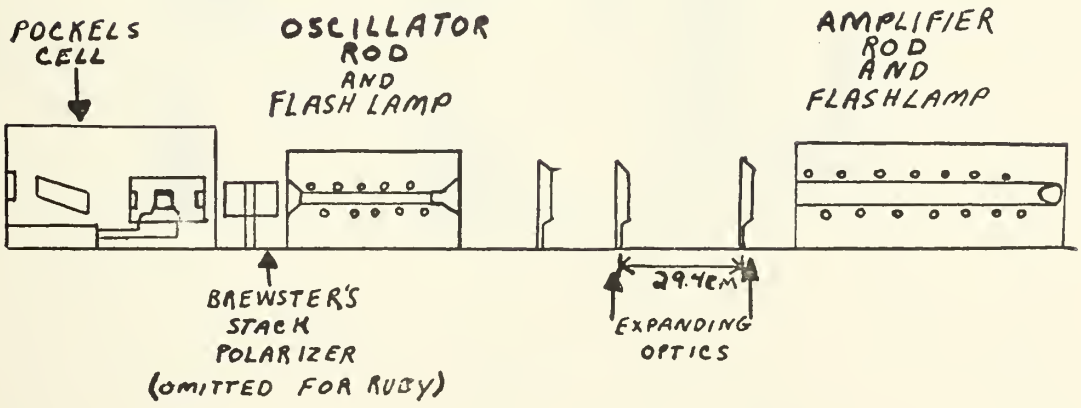

fig.6

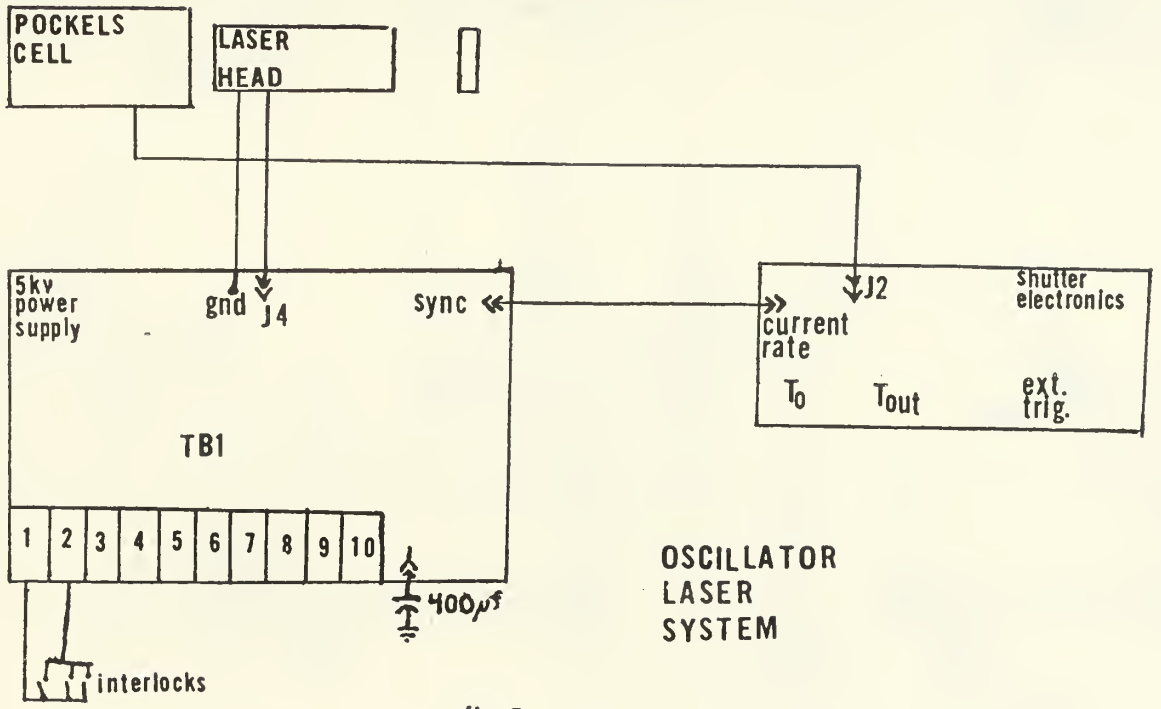
POCKELS CELL
LASER HEAD
5kv power supply
gnd
J4
sync
J2
shutter electronics
current rate
T_0
T_{out}
ext. trig.
TB1
1 2 3 4 5 6 7 8 9 10
400μf
interlocks
OSCILLATOR LASER SYSTEM

fig.7

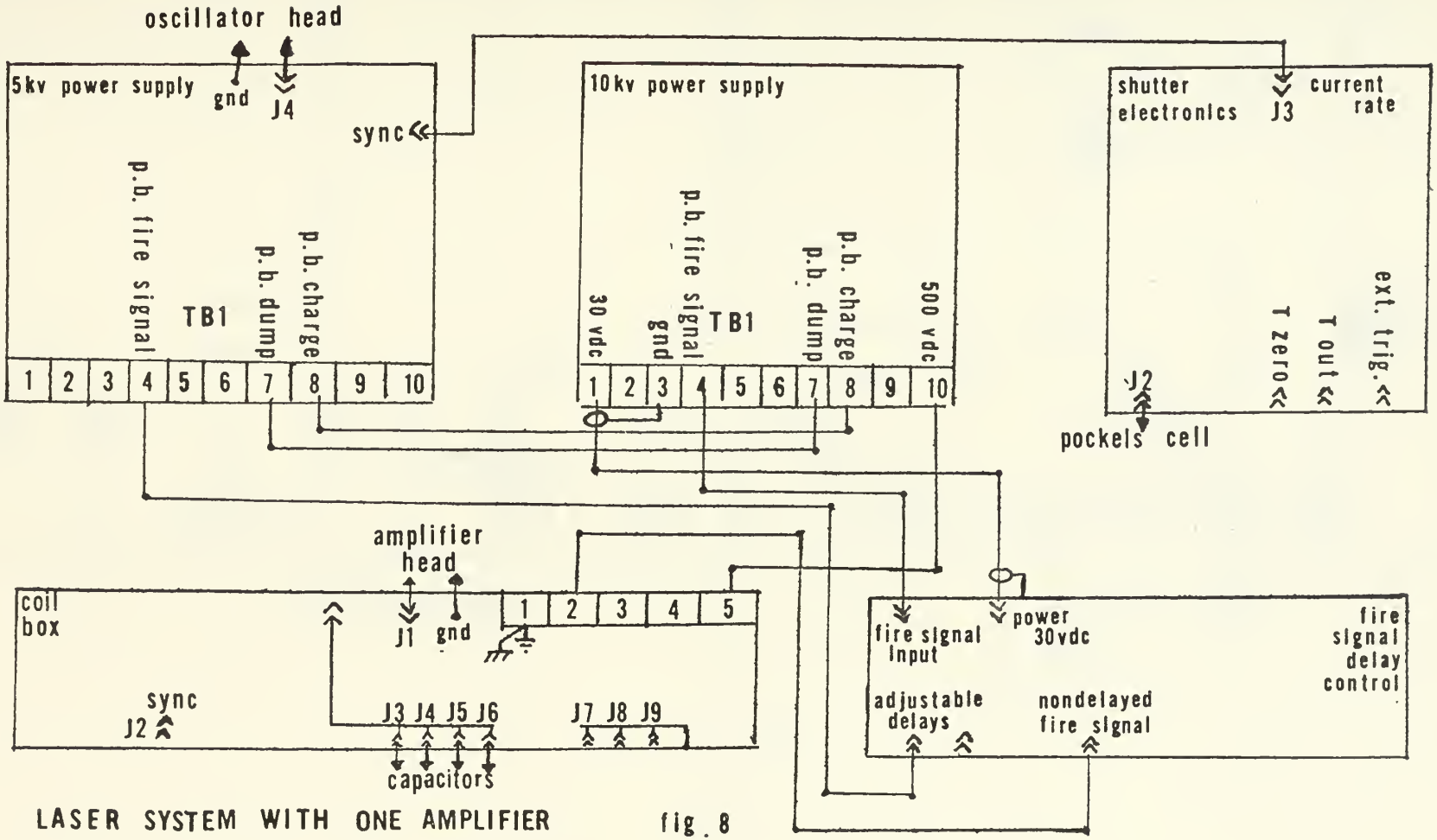

LASER SYSTEM WITH ONE AMPLIFIER fig. 8

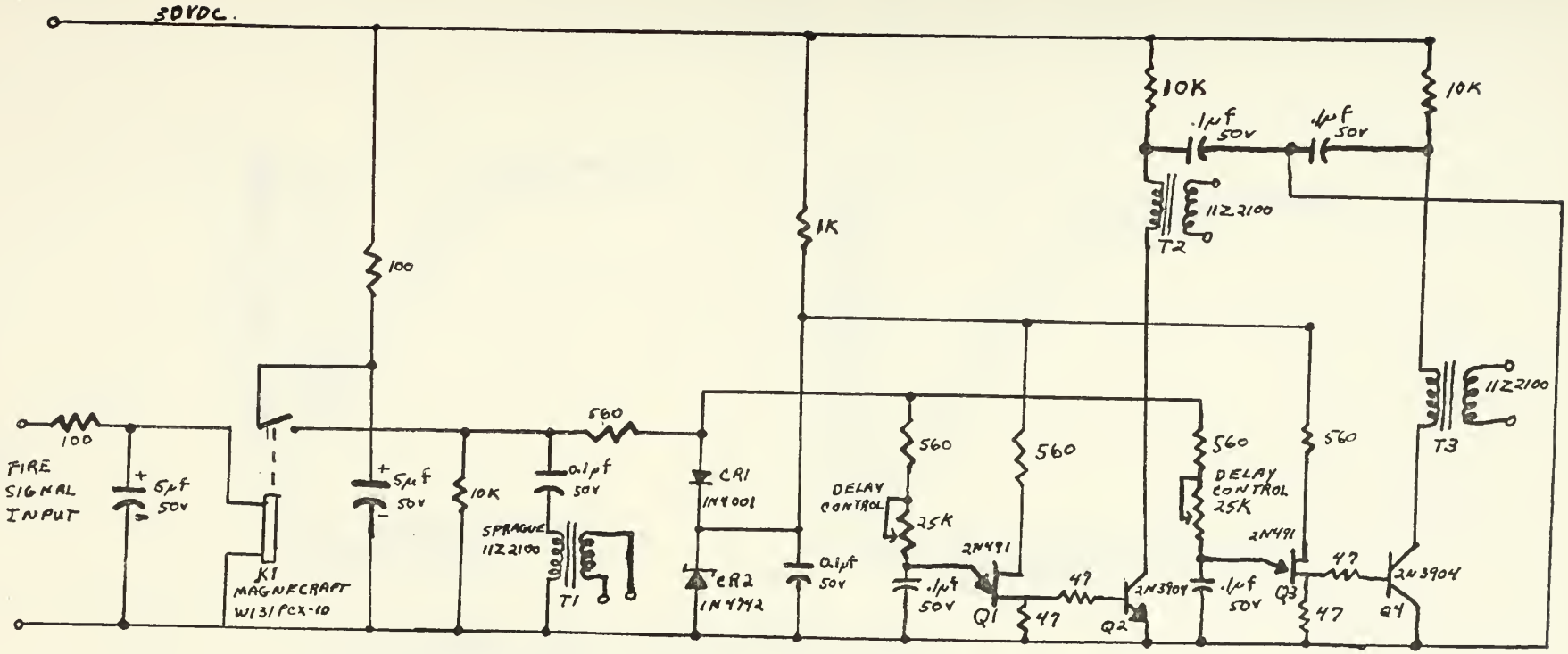

FIRE DELAY CIRCUIT

T1 nondelayed trigger
T2 delayed "
T3 " "

fig.9

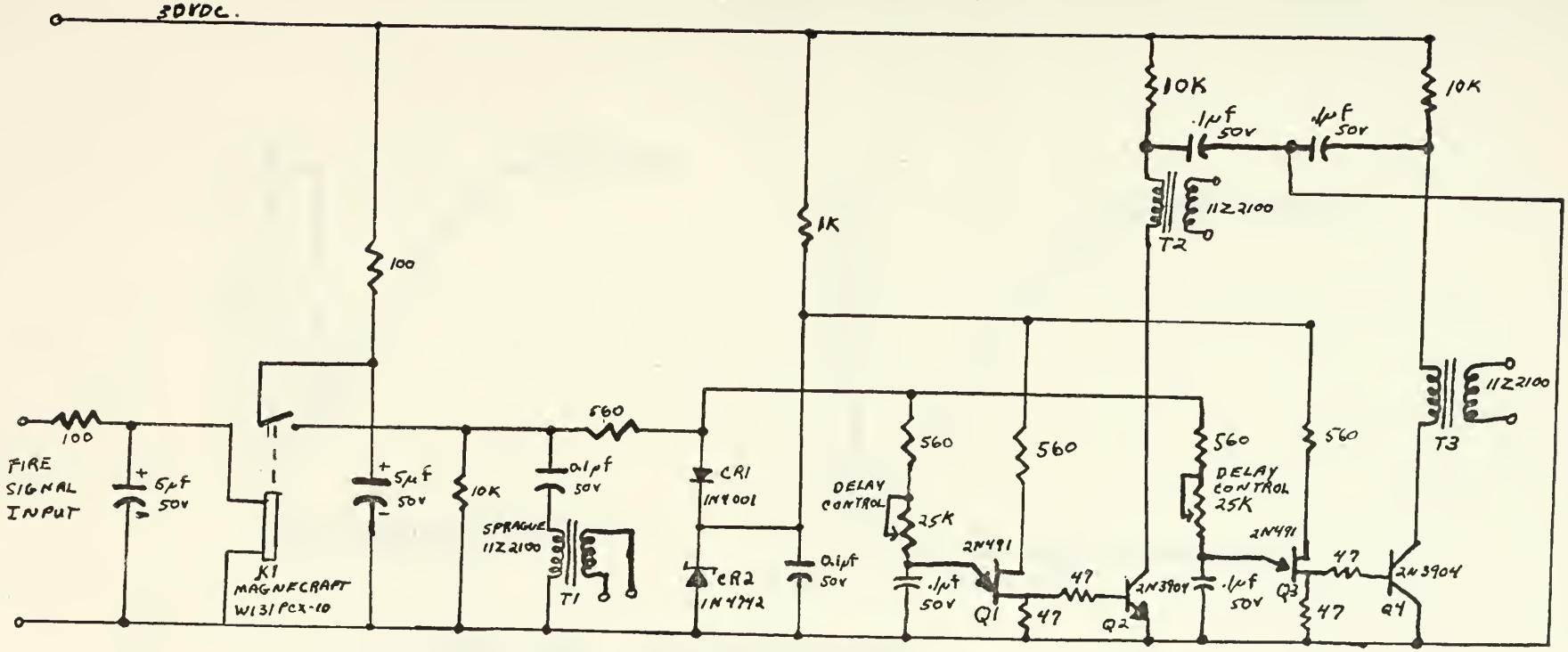

FIRE DELAY CIRCUIT

T1 nondelayed trigger
T2 delayed "
T3 " "

fig.9

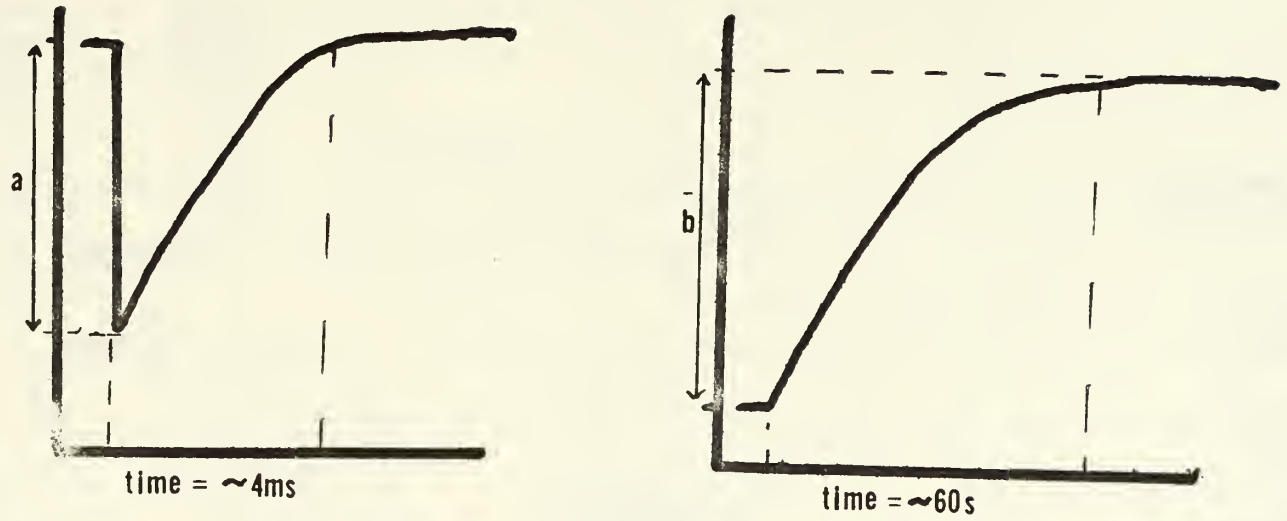

a is the detector output representing total energy

b " " calorimeter " " " "

fig.10

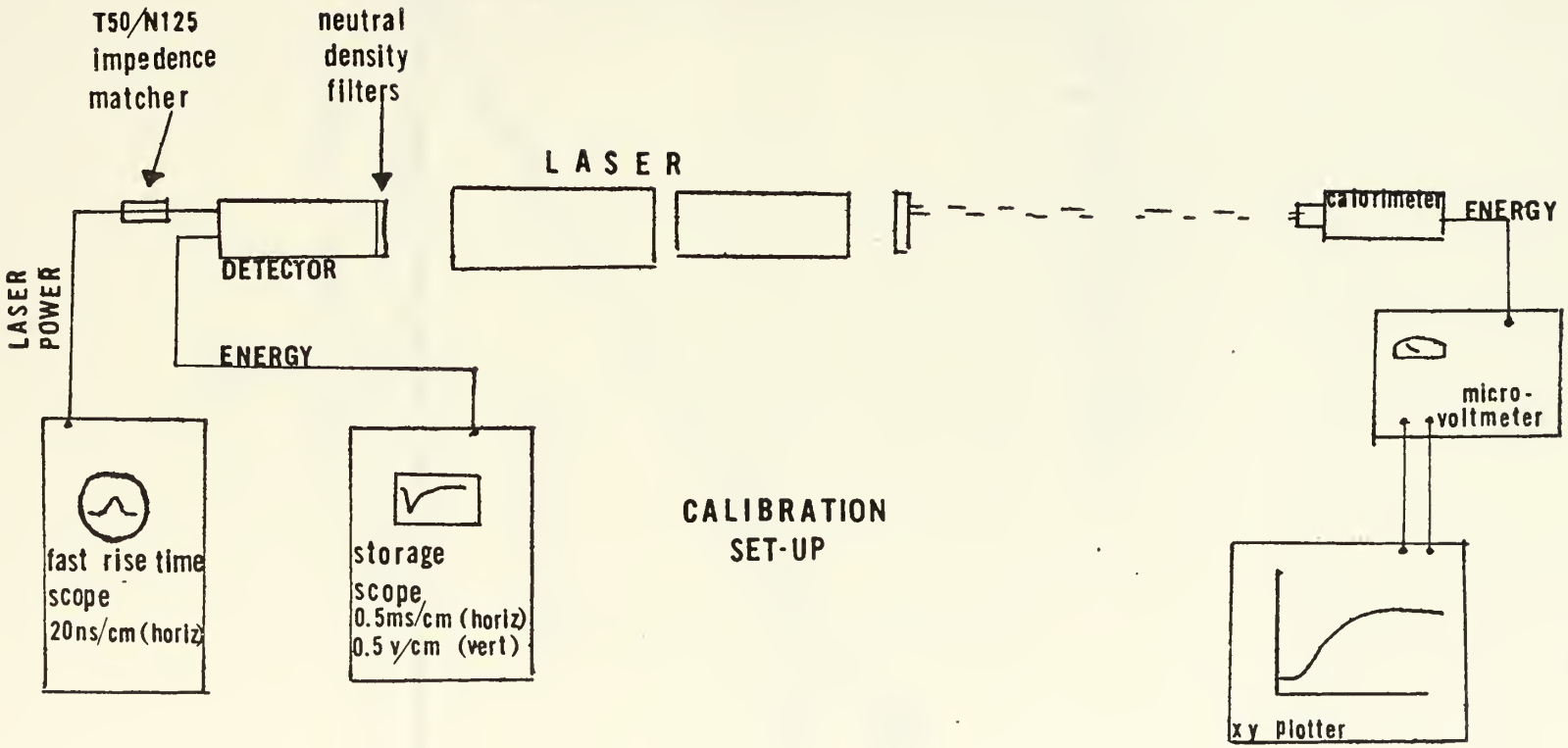
T50/N125
impedence
matcher
neutral
density
filters
LASER
calorimeter
ENERGY
DETECTOR
LASER
POWER
ENERGY
micro-
voltmeter
fast rise time
scope
20ns/cm (horiz)
storage
scope
0.5ms/cm (horiz)
0.5 v/cm (vert)
CALIBRATION
SET-UP
x y plotter

fig.II

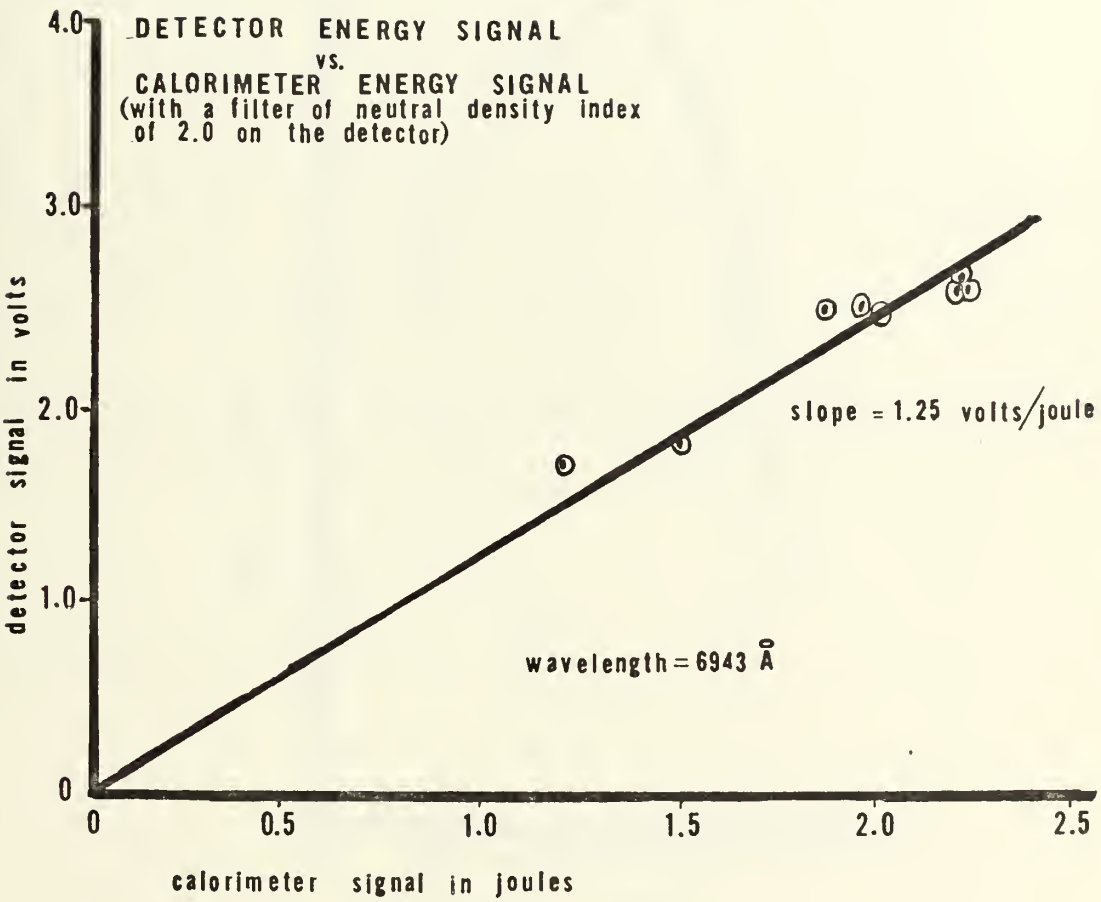
DETECTOR ENERGY SIGNAL
vs.
CALORIMETER ENERGY SIGNAL
(with a filter of neutral density index of 2.0 on the detector)
4.0
3.0
2.0
1.0
0
detector signal in volts
slope = 1.25 volts/joule
wavelength = 6943 Å
0
0.5
1.0
1.5
2.0
2.5
calorimeter signal in joules

fig.12

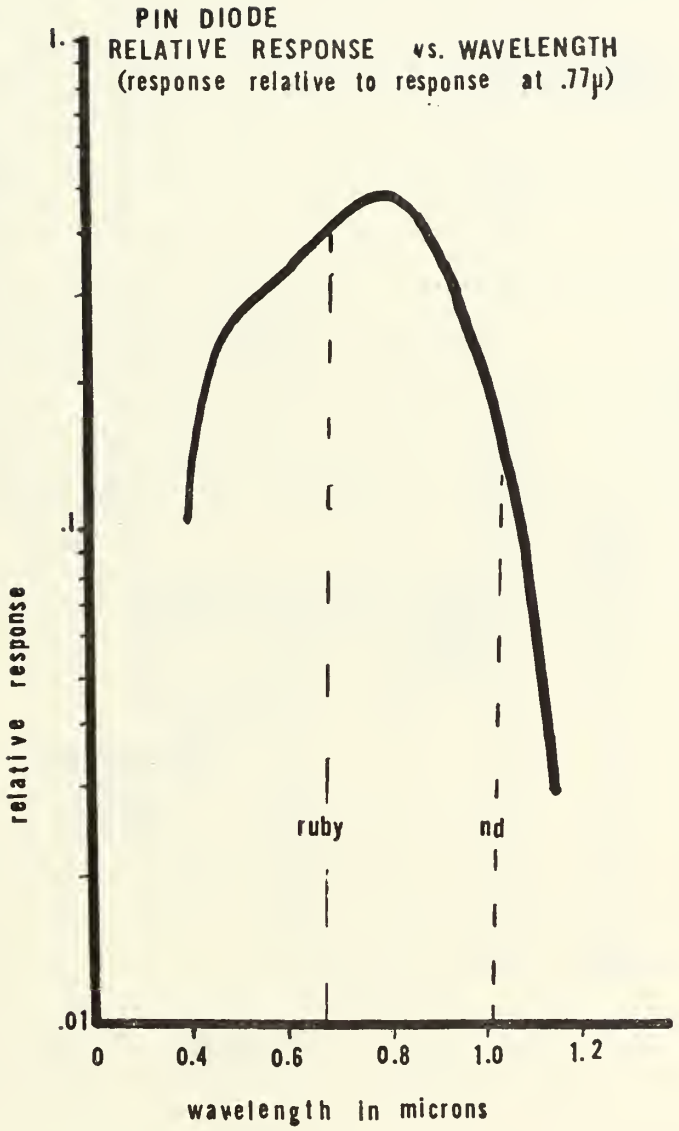
PIN DIODE
RELATIVE RESPONSE vs. WAVELENGTH
(response relative to response at .77μ)
1.
.1
.01
relative response
ruby
nd
0
0.4
0.6
0.8
1.0
1.2
wavelength in microns

fig.13

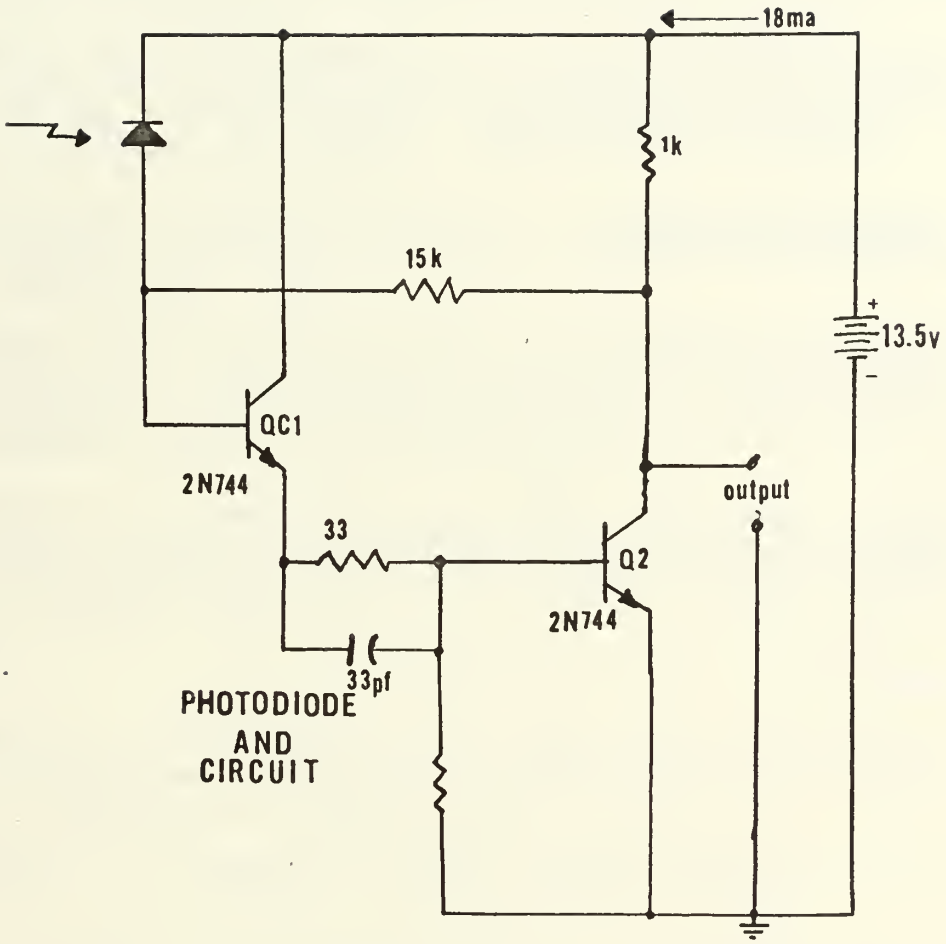
18ma
1k
15k
13.5v
QC1
2N744
output
33
Q2
2N744
33pf
PHOTODIODE
AND
CIRCUIT

fig. 14

BIBLIOGRAPHY

1. Bhadra, D. K., "Expansion of a Resistive Plasmoid in a Magnetic Field," The Physics of Fluids, v. 11, pp. 234-239, January 1968.

2. Dawson, J. M., "On the Production of Plasma by Giant Pulse Lasers," The Physics of Fluids, v. 7, pp. 981-987, July 1964.

3. Dawson, J. M. and Oberman, C., "High-Frequency Conductivity and the Emission and Absorption Coefficients of a Fully Ionized Plasma," The Physics of Fluids, v. 5, pp. 517-524, May 1962.

4. Glasstone, S. and Lovberg, R. H., Controlled Thermonuclear Reactions, pp. 29-32, 164-208, D. Van Nostrand Company, Inc., 1960.

5. Haught, A. F. and Polk, D. H., "High-Temperature Plasmas Produced by Laser Beam Irradiation of Single Solid Particles," The Physics of Fluids, v. 9, pp. 2047-2056, October 1966.

6. Haught, A. F. and Polk, D. H. and Fader, W. J., "Production of Plasmas for Thermonuclear Research by Laser Beam Irradiation of Solid Particles, "UARL F920365-6, pp. 12-24, June 1967.

7. McKee, L. L., Notes on Expanding Plasmas, Unpublished.

8. Sagdeev, R. Z., "Cooperative Phenomena in Collisionless Plasmas," Reviews of Plasma Physics, v. 4, pp. 65-68, Consultants Bureau, 1966.

9. Spitzer, L., Physics of Fully Ionized Gases, pp. 1-14, 65-88, Interscience Publishers, Inc., 1956.

10. Schwirzke, F. and Tuckfield, R. G., "Dynamics of a Laser Created Plasma Expanding in a Magnetic Field," Plasma Physics, v. 11, pp. 11-18, Pergamon Press, 1969.

11. Schwirzke, F. and Tuckfield, R. G., "Observation of Enhanced Resistivity in the Wave Front of a Laser-Produced Plasma Interacting with a Magnetic Field." Physical Review Letters, v. 22, pp. 1284-1287, June 1969.

12. Schwirzke, F., Notes on Plasma Physics, Unpublished.

13. Tanenbaum, B. S., Plasma Physics, pp. 140-148, McGraw-Hill, 1967.

INITIAL DISTRIBUTION LIST

		No. Copies
1.	Defense Documentation Center Cameron Station Alexandria, Virginia 22314	2
2.	Library, Code 0212 Naval Postgraduate School Monterey, California 93940	2
3.	Professor Fred Schwirzke, Code 61 Sw Department of Physics Naval Postgraduate School Monterey, California 93940	1
4.	LTJG Lawrence Martin Schadegg, USN c/o RADM and Mrs. R. J. Schneider 5521 Old Lawyers Hill Rd. Elkridge, Maryland 21227	1

DOCUMENT CONTROL DATA - R & D

(Security classification of title, body of abstract and indexing annotation must be entered when the overall report is classified)

1. ORIGINATING ACTIVITY *(Corporate author)*

Naval Postgraduate School
Monterey, California 93940

2a. REPORT SECURITY CLASSIFICATION

Unclassified

2b. GROUP

3 REPORT TITLE

THE DYNAMICS OF A LASER PRODUCED HEAVY ION PLASMA

4. DESCRIPTIVE NOTES *(Type of report and, inclusive dates)*

Master's Thesis; June 1970

5. AUTHOR(S) *(First name, middle initial, last name)*

Lawrence Martin Schadegg
Lieutenant (junior grade), United States Navy

6. REPORT DATE	7a. TOTAL NO. OF PAGES	7b. NO. OF REFS
June 1970	58	13

8a. CONTRACT OR GRANT NO.	9a. ORIGINATOR'S REPORT NUMBER(S)
b. PROJECT NO.	
c.	9b. OTHER REPORT NO(S) *(Any other numbers that may be assigned this report)*
d.	

10. DISTRIBUTION STATEMENT

This document has been approved for public release and sale; its distribution is unlimited.

11. SUPPLEMENTARY NOTES	12. SPONSORING MILITARY ACTIVITY
	Naval Postgraduate School Monterey, California 93940

13. ABSTRACT

To investigate the front of a laser produced plasma that is expanding in a homogeneous magnetic field a reliable method of positioning the target, monitoring the laser, and observing the properties of the expanding plasma had to be developed. Photodiodes and supporting circuitry were constructed to observe the laser interaction with the plasma, plasma expansion velocity, and total light emitted from the plasma. A heavy material, copper, was chosen to slow down the processes occurring in the expanding plasma front.

The predictions of a computer program of the mathematical analogue to the experiment give expansion velocities of $\sim 10^6$ cm/sec and indicate a bouncing of the plasma front off the magnetic field.

KEY WORDS	LINK A		LINK B		LINK C	
	ROLE	WT	ROLE	WT	ROLE	WT
Laser Produced Plasma						